

ARTICLES

Multistep Thermal Relaxation of Photoisomers in Polyphotochromic Molecules

Jérôme Berthet, Jean-Claude Micheau,[†] Anatoli Metelitsa,[‡] Gaston Vermeersch, and Stéphanie Delbaere*

Laboratoire de Physique, UMR CNRS 8009, Faculté de Pharmacie, Université de Lille 2, BP 83, 59006 Lille Cedex, France

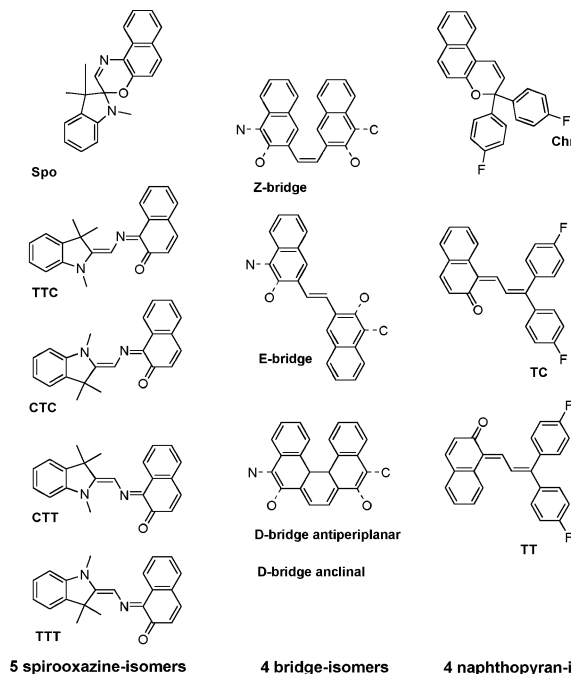
Received: July 15, 2004; In Final Form: October 5, 2004

UV irradiation of a polyphotochromic molecule bearing a spirooxazine unit linked to a naphthopyran by a Z-ethenic bridge produces several interconverting nonequilibrium dihydrophenanthrenic photocyclized isomers. A quantitative kinetic analysis of the thermal evolution after photocyclization has been performed using ¹H and ¹⁹F NMR spectroscopy at different temperatures. Spirooxazine (Spo) ring opening and TTC/CTC (i.e., trans–transoid–cis/cis–transoid–cis) isomerization occur reversibly, but only when the naphthopyran ring is closed. In contrast, naphthopyran ring opening is irreversible and is observed when the spirooxazine ring is either closed or open in the TTC configuration, but not from the CTC configuration. Activation parameters of the main isomerization processes have been determined. Relative stability of the various isomers (TTC > CTC > Spo) has been established. The use of model compounds bearing either a spirooxazine or a naphthopyran in a similar dihydrophenanthrenic environment confirms these specific reactivities and relative stabilities in accordance with PM-3 calculations.

Introduction

Organic photochromic molecules whose structure and macroscopic properties can be controlled by light irradiation are of considerable interest due to their potential applications in optical memory media and photoswitching devices.^{1–6} Among photochromic families, spirooxazine^{7,8} and naphthopyran^{9,10} (3H-chromenes) have been extensively studied due to their good colorability, fast thermal bleaching, and high fatigue resistance. Such photochromism exhibits a simple binary open vs closed behavior. However, much more complex systems can be obtained by combining two or more photochromic units. The first examples were reported as far back as 1966 by Gautron¹¹ and 1972 by Guglielmetti¹² by linking two spiropyran units with a paraffin chain. However, the lack of novel molecules has impeded their development until recent years¹³ during which the use of modern analytical techniques has unveiled an unprecedented wealth of behavior. For instance, by linking a spirooxazine unit to a naphthopyran unit by a Z-ethenic bridge, a polyphotochromic molecule has been synthesized.^{14,15} It is expected that under UV irradiation, such a molecule can give rise to a relatively large number of photoisomers (Scheme 1).

Until now, preliminary studies^{19,20} have identified some photoisomers whose relative proportions depend on the temperature and duration of irradiation. Besides the structural complexity of such mixtures, thermal evolution after irradiation has also been recorded. Molecules keeping the ethenic bridge

SCHEME 1: Structures of All the Theoretically Possible Photoisomers of Spo-Z-Chr^a

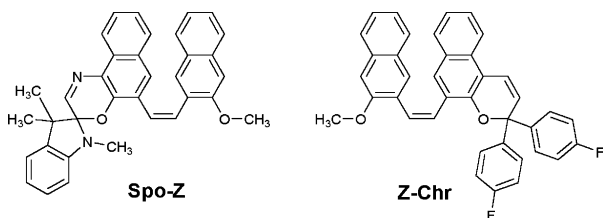
^a As there are 5 spirooxazine-photoisomers (Spo, TTC, CTC, CTT and TTT),¹⁶ 4 bridge-photoisomers (Z, E, cyclized antiperiplanar and cyclized ancinal),¹⁷ and 3 naphthopyran-photoisomers (Chr, TC and TT),¹⁸ no less than 60 photoisomers are theoretically expected.

in either the Z or the E configuration undergo the expected reversible closing of the open spirooxazine and naphthopyran

* Corresponding author. E-mail: sdelbaer@pharma.univ-lille2.fr. Fax: 33 3 2095 9009. Tel: 33 3 2090 4013.

[†] Laboratoire IMRCP, UMR CNRS 5623, Université Paul Sabatier, 31062 Toulouse, France.

[‡] Institute of Physical and Organic Chemistry, Rostov University, 344090 Rostov on Don, Russia.

SCHEME 2: Structures of the Spo-Z and Z-Chr Model Compounds

units. In contrast, photocyclized molecules bearing a dihydrophenanthrene (or D-bridge) show a much more complex kinetic behavior with irreversible and reversible slow color development and temperature sensitivity (thermochromism).²¹

The purpose of this paper is to perform a kinetic analysis of such light-driven complex molecular systems using multinuclear NMR monitoring techniques.²² From the ¹H and ¹⁹F NMR experimental kinetic curves recorded at different temperatures after UV irradiation, we have analyzed the dark multistep isomerization processes occurring between the photocyclized isomers of Spo-Z-Chr. Moreover, to facilitate the kinetic analysis of such an intricate network, two model compounds exhibiting a similar environment (Spo-Z and Z-Chr; Scheme 2) have also been investigated under the same conditions.

It has been demonstrated that among all the possible isomers only some of them accumulate significantly. Moreover, we have also shown that among all the expected isomerization pathways connecting these isomers, only a few of them are really efficient. The relative stability of the various isomers has been estimated from experimental free enthalpy determinations and PM3 calculations.

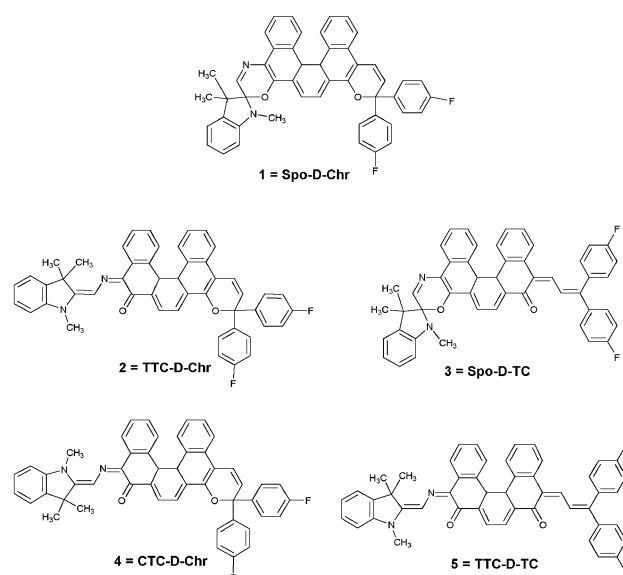
Experimental Section

Irradiation. Samples (5×10^{-3} M in toluene-*d*₈) were irradiated in NMR tubes (5 mm) at different temperatures in a home-built apparatus that has been previously described.²³ The emission spectrum of a 1000-W Xe-Hg high-pressure filtered (Schott 011FG09: $259 < \lambda < 388$ nm with $\lambda_{\text{max}} = 330$ nm and $T = 79\%$) short-arc lamp (Oriel), was focused on the end of a silica light-pipe (length 6 cm, diameter 8 mm), leading the light to the spinning sample tube, inserted in a quartz dewar. The temperature of the sample was controlled with a variable temperature unit (B-VT1000-Bruker, 123–423 K, T range). The time of irradiation was adjusted between 5 (at 273 K) and 30 min (at 234 K). Typical photocyclization conversions were around 45% for Spo-Z-Chr and 20% for Z-Chr and Spo-Z.

¹H and ¹⁹F NMR. After irradiation, the tube was transferred into the NMR probe of a Bruker DPX 300 spectrometer (¹H 300 MHz and ¹⁹F 282 MHz). To monitor photo-cyclization, the spectra were recorded at regular time intervals. ¹⁹F NMR resonances²⁴ were used for D-Chr and Spo-D-Chr, while the ¹H (N-CH₃) signal was monitored for Spo-D.²⁵ The concentration of each photocyclized product was obtained from the ratio of peak intensities.

Fitting Procedure. Homemade software^{26–28} was used to perform curve fittings. Although in such first-order kinetic networks the use of analytical expressions of the evolution of concentrations was possible,²⁹ their expression became rapidly cumbersome when the number of reversible processes and isomers increased. Hence, the differential equations were integrated using a classical 4th order Runge–Kutta method.

PM-3 Calculations. Semiempirical quantum-chemical calculations were carried-out using the PM-3 method with the

SCHEME 3: Photoisomers of Spo-Z-Chr Bearing a Dihydrophenanthrenic Bridge (D-bridge)

MOPAC program.³⁰ Thermodynamic stabilities in solution were estimated using the AMSOL 6.6 program package.³¹ The SM5.4/PM-3 solvation model was used for the present calculations.

Results and Discussion

Depending on the irradiation conditions (temperature and duration), the polyphotochromic molecule Spo-Z-Chr undergoes several isomerizations of its three photochromic units. Among them, photocyclization of the Z-ethenic bridge into a dihydrophenanthrenic configuration (D-bridge) gives rise to a series of thermochromic isomers (Scheme 3). The closed–closed Spo-D-Chr (1), three open–closed TTC-D-Chr (2), Spo-D-TC (3), and CTC-D-Chr (4) structures, and one open–open TTC-D-TC (5) structure were characterized from NMR investigations (Figure 1).^{32,33} The other expected isomers: Spo-D-TT, TTC-D-TT, CTC-D-TT, and CTC-D-TC were not observed.

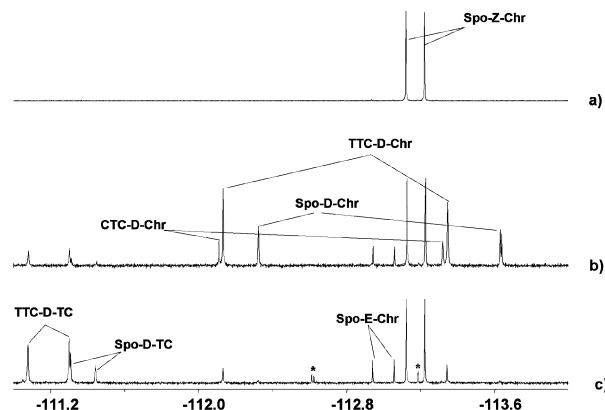


Figure 1. Part of ¹⁹F NMR spectra of Spo-Z-Chr in toluene (a) before *hν*, (b) after *hν*, and (c) 14 h after *hν* at 253 K (*degradation products).

Kinetic Analysis of the Multistep Thermal Isomerization of the Set of Photocyclized Isomers Obtained After Spo-Z-Chr UV Irradiation. Owing to their nonequilibrium state following UV irradiation, the whole set of photocyclized isomers undergoes a multistep relaxation process toward a new equilibrium position. The concentration vs time profile of each

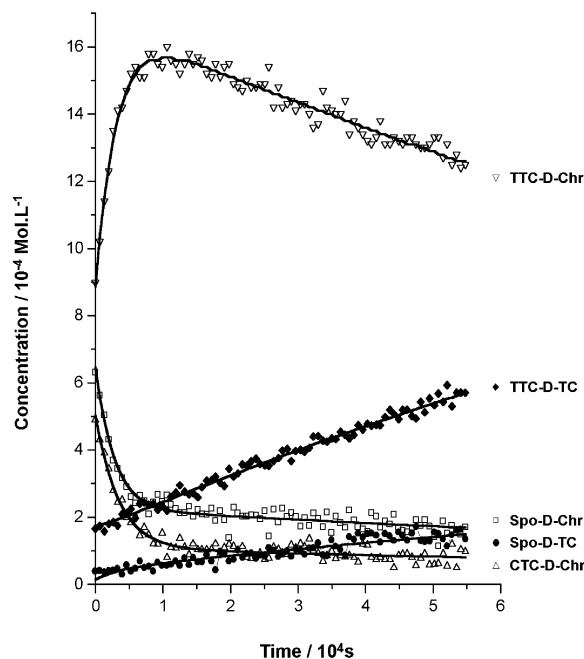
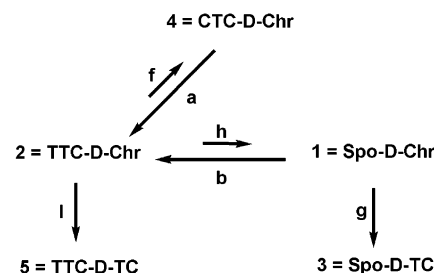


Figure 2. Dark evolution of the concentrations of the five photocyclized isomers obtained after UV irradiation of Spo-Z-Chr at 253 K. Symbols are experimental data; continuous lines are fitted curves from the model.

photocyclized isomer, obtained from the measurements of peak-intensities in ^{19}F NMR spectra, is presented in Figure 2.

Rapid examination of the kinetic curves shows that Spo-D-Chr (1), TTC-D-Chr (2), and CTC-D-Chr (4) exhibit a biexponential-like behavior with “brief” ($\sim 10^{-5}\text{s}^{-1}$) and “slow” ($\sim 10^{-6}\text{s}^{-1}$) time constants. Moreover, Spo-D-Chr (1) and CTC-D-Chr (4) decrease rapidly while TTC-D-Chr (2) increases rapidly at an equivalent rate. Then, the three isomers (1), (2), and (4) decrease slowly. Simultaneously, the two compounds with the naphthopyran unit open (Spo-D-TC (3) and TTC-D-TC (5)) increase slowly in a monotonic way. It is likely that these two compounds come, respectively, from Spo-D-Chr (1) and TTC-D-Chr (2). Taking into account the least-motion principle, not all the isomerization processes are expected to occur. We considered that only structures that are changed by the isomerization of a single unit are connected. As a consequence we have excluded the isomerization paths between 3 and 2, 3 and 4, 5 and 4, and 5 and 1. Six isomerization paths between 1 and 2, 1 and 3, 2 and 5, 3 and 5, 4 and 2, and 4 and 1 remained to be determined. They involved 12 independent rate constants: k_{12} , k_{21} , k_{13} , k_{31} , k_{25} , k_{52} , k_{35} , k_{53} , k_{24} , k_{42} , k_{14} , and k_{41} . To determine their experimental values, the whole set

SCHEME 4: Isomerization Path Network between the Five Isomers^a



^a Long arrows are intended to represent the more rapid processes, while shorter arrows are for the slower ones. Letters refer to Tables 2 and 5.

of kinetic curves was submitted to kinetic modeling using a set of linear differential equations:

$$\frac{d[i]}{dt} = -[i] \cdot \sum_m k_{im} + \sum_m k_{mi}[m] \quad (i \neq m) \quad (1)$$

where $i = 1, 2, 3, 4$, or 5 and m is the list of species with which the species i is connected.

Table 1 is intended to illustrate the method by showing the values of the residual least-squares χ^2 for different sets of rate constants. This example is applied to data corresponding to Figure 2. To start, all the rate constants are arbitrarily set at $5 \times 10^{-6}\text{s}^{-1}$ (step 0) giving rise to a high χ^2 ($1.77 \cdot 10^{-7}$), then during steps 1 and 2, these values were automatically adjusted to decrease the χ^2 (step 1) then to decrease more (step 2). This result was considered as an acceptable fit. Examination of the results after step 2 shows that some values (k_{31} , k_{52} , k_{35} , k_{53} , k_{14} , and k_{41}) remained 1 or 2 orders of magnitude smaller than the others. Step 3 shows that all the smallest rate constants can be neglected without any loss of fitting quality. On the other hand, steps 4 and 5 show that removal of one of the selected processes destroys the fit, which cannot be recovered even if the nonsignificant paths are reintroduced (step 6). Moreover, it was shown that, whatever the starting conditions, the same processes with the same rate constant values were selected.

During the fitting procedure, it was shown that the magnitude of several rate constants is 2 orders of magnitude smaller than the rest. They could be canceled without any loss of fitting accuracy. The following kinetic network (Scheme 4) was obtained, involving only k_{12} , k_{21} , k_{24} , k_{42} , k_{13} , and k_{25} .

Two unexpected results were found. (i) There is no significant isomerization between CTC-D-Chr (4) and Spo-D-Chr (1). (ii) The formation of the TC open naphthopyran is irreversible and does not occur from the CTC isomer; there is no TT formation.

TABLE 1: Calculated Rate Constants and χ^2 Values during the Step by Step Fitting Procedure of Data from Spo-D-Chr at 253K (Best Fit Is at Step 3)

process		step 0	step 1	step 2	step 3	step 4	step 5	step 6
Spo-D-Chr \rightarrow TTC-D-Chr	k_{12}	$5.0 \cdot 10^{-6}$	$1.5 \cdot 10^{-4}$	$2.4 \cdot 10^{-4}$	$2.4 \cdot 10^{-4}$	$2.2 \cdot 10^{-4}$	$3.2 \cdot 10^{-4}$	
TTC-D-Chr \rightarrow Spo-D-Chr	k_{21}	$5.0 \cdot 10^{-6}$	$1.5 \cdot 10^{-5}$	$1.7 \cdot 10^{-5}$	$1.7 \cdot 10^{-5}$		$3.6 \cdot 10^{-5}$	$2.6 \cdot 10^{-5}$
Spo-D-Chr \rightarrow Spo-D-TC	k_{13}	$5.0 \cdot 10^{-6}$	$3.8 \cdot 10^{-5}$	$2.1 \cdot 10^{-5}$	$2.1 \cdot 10^{-5}$	$2.4 \cdot 10^{-5}$	$2.7 \cdot 10^{-5}$	$2.1 \cdot 10^{-5}$
Spo-D-TC \rightarrow Spo-D-Chr	k_{31}	$5.0 \cdot 10^{-6}$	$1.3 \cdot 10^{-5}$	$1.6 \cdot 10^{-7}$				
TTC-D-Chr \rightarrow TTC-D-TC	k_{25}	$5.0 \cdot 10^{-6}$	$2.4 \cdot 10^{-5}$	$5.1 \cdot 10^{-6}$	$5.1 \cdot 10^{-6}$	$6.1 \cdot 10^{-6}$		$9.4 \cdot 10^{-6}$
TTC-D-TC \rightarrow TTC-D-Chr	k_{52}	$5.0 \cdot 10^{-6}$	$8.2 \cdot 10^{-5}$	$7.7 \cdot 10^{-8}$				
Spo-D-TC \rightarrow TTC-D-TC	k_{35}	$5.0 \cdot 10^{-6}$	$5.5 \cdot 10^{-5}$	$3.3 \cdot 10^{-7}$				
TTC-D-TC \rightarrow Spo-D-TC	k_{53}	$5.0 \cdot 10^{-6}$	$1.8 \cdot 10^{-5}$	$1.3 \cdot 10^{-7}$				
CTC-D-Chr \rightarrow TTC-D-Chr	k_{42}	$5.0 \cdot 10^{-6}$	$3.4 \cdot 10^{-4}$	$2.9 \cdot 10^{-4}$	$2.9 \cdot 10^{-4}$	$2.9 \cdot 10^{-4}$	$3.4 \cdot 10^{-4}$	$2.9 \cdot 10^{-4}$
TTC-D-Chr \rightarrow CTC-D-Chr	k_{24}	$5.0 \cdot 10^{-6}$	$4.1 \cdot 10^{-5}$	$3.8 \cdot 10^{-5}$	$3.8 \cdot 10^{-5}$	$3.9 \cdot 10^{-5}$	$5.7 \cdot 10^{-5}$	$2.2 \cdot 10^{-5}$
Spo-D-Chr \rightarrow CTC-D-Chr	k_{14}	$5.0 \cdot 10^{-6}$	$8.5 \cdot 10^{-5}$	$1.6 \cdot 10^{-7}$				$2.4 \cdot 10^{-6}$
CTC-D-Chr \rightarrow Spo-D-Chr	k_{41}	$5.0 \cdot 10^{-6}$	$6.9 \cdot 10^{-5}$	$1.7 \cdot 10^{-7}$				
	χ^2	$1.7 \cdot 10^{-7}$	$2.2 \cdot 10^{-9}$	$3.7 \cdot 10^{-10}$	$3.7 \cdot 10^{-10}$	$2.1 \cdot 10^{-9}$	$1.4 \cdot 10^{-8}$	$2.1 \cdot 10^{-8}$

TABLE 2: Calculated Rate Constants of the Selected Isomerization Process of Spo-D-Chr at Various Temperatures and χ^2 Values of the Fitting^a

T (K)	243	249	253	259	263	273
Spo-D-Chr \rightarrow TTC-D-Chr (b)	$9.0 \cdot 10^{-5}$	$1.5 \cdot 10^{-4}$	$2.4 \cdot 10^{-4}$	$3.7 \cdot 10^{-4}$	$6.2 \cdot 10^{-4}$	$1.8 \cdot 10^{-3}$
TTC-D-Chr \rightarrow Spo-D-Chr (h)	$6.4 \cdot 10^{-6}$	$1.1 \cdot 10^{-5}$	$1.6 \cdot 10^{-5}$	$2.4 \cdot 10^{-5}$	$4.2 \cdot 10^{-5}$	$1.6 \cdot 10^{-4}$
TTC-D-Chr \rightarrow CTC-D-Chr (f)	$1.1 \cdot 10^{-5}$	$2.1 \cdot 10^{-5}$	$3.8 \cdot 10^{-5}$	$4.9 \cdot 10^{-5}$	$5.7 \cdot 10^{-5}$	$1.4 \cdot 10^{-4}$
CTC-D-Chr \rightarrow TTC-D-Chr (a)	$8.3 \cdot 10^{-5}$	$1.8 \cdot 10^{-4}$	$2.9 \cdot 10^{-4}$	$4.3 \cdot 10^{-4}$	$6.4 \cdot 10^{-4}$	$1.3 \cdot 10^{-3}$
Spo-D-Chr \rightarrow Spo-D-TC (g)	<i>m</i>	$1.3 \cdot 10^{-5}$	$2.1 \cdot 10^{-5}$	$7.2 \cdot 10^{-5}$	$1.1 \cdot 10^{-4}$	$2.9 \cdot 10^{-4}$
TTC-D-Chr \rightarrow TTC-D-TC (l)	<i>m</i>	$1.8 \cdot 10^{-6}$	$5.1 \cdot 10^{-6}$	$9.9 \cdot 10^{-6}$	$1.9 \cdot 10^{-5}$	$7.3 \cdot 10^{-5}$
χ^2	$1.3 \cdot 10^{-9}$	$4.9 \cdot 10^{-10}$	$3.7 \cdot 10^{-10}$	$7.0 \cdot 10^{-10}$	$6.2 \cdot 10^{-10}$	$2.9 \cdot 10^{-10}$

^a *m*: These slow processes have not been detected at the lowest temperature because their contribution to the whole relaxation was negligible.

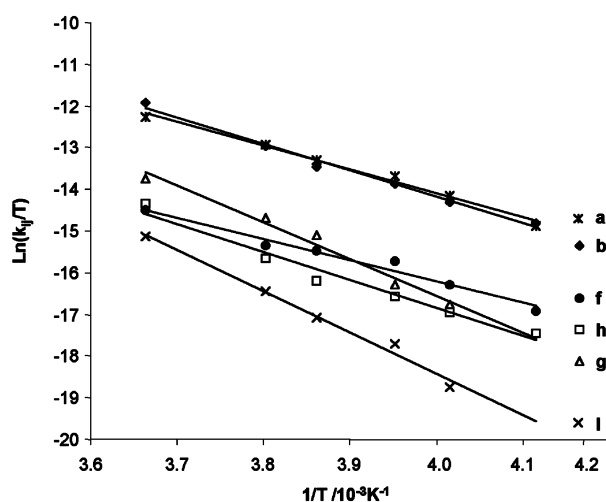
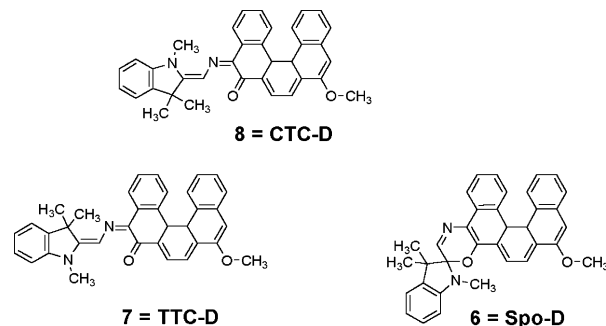


Figure 3. Eyring plots for the six thermal processes of the Spo-D-Chr system: (a) CTC-D-Chr \rightarrow TTC-D-Chr; (b) Spo-D-Chr \rightarrow TTC-D-Chr; (f) TTC-D-Chr \rightarrow CTC-D-Chr; (h) TTC-D-Chr \rightarrow Spo-D-Chr; (g) Spo-D-Chr \rightarrow Spo-D-TC; (l) TTC-D-Chr \rightarrow TTC-D-TC.

SCHEME 5: Photoisomers of Spo-Z Bearing a Dihydrophenanthrenic Bridge (D-bridge)



These rate constants were determined at six different temperatures from 243 to 273 K (Table 2). Their accuracy was sufficient to estimate the enthalpy and entropy of activation, ΔH^\ddagger and ΔS^\ddagger of each of the six isomerization processes using Eyring's equation³⁴ by plotting $\text{Ln}(k_{ij}/T)$ vs $1/T$ (Figure 3). The activation parameters will be discussed below. The use of model compounds in which either a spirooxazine or a naphthopyran unit has been removed fully confirms these conclusions.

Kinetic Analysis of the Thermal Relaxation of the Set of Photoisomers Obtained After Spo-Z UV Irradiation. UV irradiation of the model molecule Spo-Z leads to the formation of three photocyclized structures, which were identified as the closed isomer Spo-D (6) and its trans-transoid-cis TTC-D (7) and cis-transoid-cis CTC-D (8) photomerocyanines (Scheme 5).³⁵

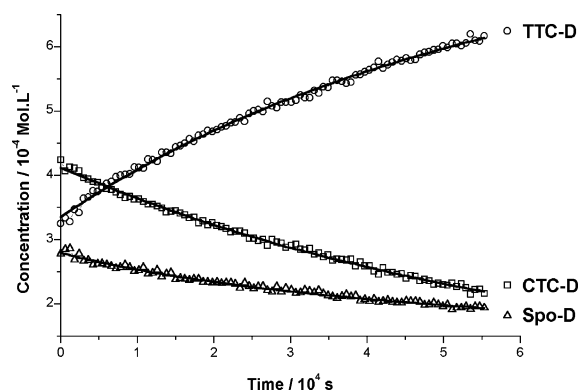
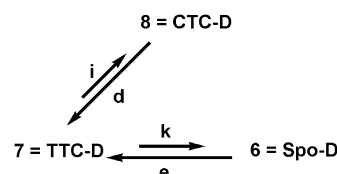


Figure 4. Thermal evolution at 234 K of the three cyclized photoisomers obtained from irradiation of Spo-Z. Signs are experimental data; continuous lines are fitted curves from the model (see Scheme 6).

SCHEME 6: Mechanistic Model of the Interconversion Paths between the Three Cyclized Isomers of Spo-Z^a



^a Letters refer to Tables 3 and 5.

Kinetic analysis of time-evolution of the concentrations after UV irradiation (Figure 4) indicates the existence of two consecutive reversible reactions linking the open merocyanine TTC-D (7) with the closed Spo-D (6) and with its isomer CTC-D (8).

Comparison of Schemes 4 and 6 shows that the spirooxazine unit behaves similarly in either Spo-D-Chr (1) or Spo-D (6) model compounds. The analysis performed at seven temperatures ranging from 234 to 263 K confirms the lack of isomerization between CTC-D and Spo-D isomers (Table 3). As previously, the activation parameters were determined (see Supporting Information) and will be discussed below.

Kinetic Analysis of the Thermal Isomerization of the Set of Photoisomers Obtained After Z-Chr UV Irradiation. After UV irradiation of Z-Chr,³⁶ three photocyclized compounds were obtained and identified: the antiperiplanar D_{ap} -Chr (9) and the anticlinal D_{ac} -Chr (10), both exhibiting naphthopyran in its closed form, and D-TC (11) with open naphthopyran (Scheme 7). This result was surprising because such antiperiplanar vs anticlinal isomerism had not been seen within previous systems.

The kinetics were recorded using ¹⁹F NMR spectroscopy. The plots (Figure 5) show that D_{ap} -Chr undergoes a first-order irreversible decrease, while its conformer, D_{ac} -Chr, follows a biexponential-like evolution first increasing then decreasing

TABLE 3: Calculated Rate Constants of the Selected Processes of Spo-D Isomerization at Various Temperatures and χ^2 Values of the Fittings^a

<i>T</i> (K)	234	239	243	249	253	259	263
Spo-D → TTC-D (e)	1.4 10 ⁻⁵	1.9 10 ⁻⁵	4.9 10 ⁻⁵	1.4 10 ⁻⁴	1.9 10 ⁻⁴	3.5 10 ⁻⁴	7.1 10 ⁻⁴
TTC-D → Spo-D (k)	<i>m</i>	1.2 10 ⁻⁶	1.8 10 ⁻⁶	6.1 10 ⁻⁶	7.0 10 ⁻⁶	1.1 10 ⁻⁵	1.9 10 ⁻⁵
CTC-D → TTC-D (d)	1.4 10 ⁻⁵	2.7 10 ⁻⁵	6.1 10 ⁻⁵	1.4 10 ⁻⁴	2.1 10 ⁻⁴	3.8 10 ⁻⁴	5.8 10 ⁻⁴
TTC-D → CTC-D (i)	1.2 10 ⁻⁶	1.6 10 ⁻⁶	3.2 10 ⁻⁶	5.9 10 ⁻⁶	1.3 10 ⁻⁵	2.4 10 ⁻⁵	4.0 10 ⁻⁵
χ^2	1.58 10 ⁻¹¹	1.52 10 ⁻¹¹	4.94 10 ⁻¹¹	5.39 10 ⁻¹¹	7.95 10 ⁻¹¹	2.49 10 ⁻¹¹	3.92 10 ⁻¹¹

^a *m*: These slow processes have not been detected at the lowest temperature because their contribution to the whole relaxation was negligible.

TABLE 4: Calculated Rate Constants of the Selected Processes of D-Chr Isomerization at Various Temperatures and χ^2 Values of the Fittings

<i>T</i> (K)	248	253	258	263	268	273
D _{ap} -Chr → D _{ac} -Chr (c)	1.1 10 ⁻⁴	2.3 10 ⁻⁴	7.2 10 ⁻⁴	1.9 10 ⁻³	<i>p</i>	<i>p</i>
D _{ac} -Chr → TC-D (j)	4.1 10 ⁻⁶	1.1 10 ⁻⁵	2.4 10 ⁻⁵	6.7 10 ⁻⁵	8.1 10 ⁻⁵	1.9 10 ⁻⁴
χ^2	5.5 10 ⁻¹¹	3.2 10 ⁻¹¹	5.6 10 ⁻¹¹	7.5 10 ⁻¹¹	1.1 10 ⁻¹⁰	9.3 10 ⁻¹¹

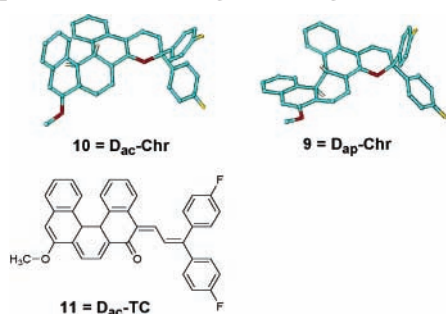
^a *p*: It is likely that at these higher temperatures this fast process was already relaxed before the start of the monitoring, hence it has not been detected.

TABLE 5: Activation Parameters of the Various Processes in Spo-D-Chr, Spo-D, and Chr-D Classified According to Increasing Values of Their Free Enthalpies of Activation (ΔG^\ddagger at 250 K), Hence the Faster Are at the Top^a

row	kinetic process	<i>r</i> ²	ΔH^\ddagger (kJ·mol ⁻¹)	ΔS^\ddagger (J·mol ⁻¹ ·K ⁻¹)	ΔG^\ddagger (kJ·mol ⁻¹)
a	CTC-D-Chr → TTC-D-Chr	0.987	51.2 ± 1.3	-110.4 ± 6.1	78.8 ± 3.4
b	Spo-D-Chr → TTC-D-Chr	0.992	52.5 ± 2.1	-105.8 ± 9.6	79.0 ± 4.0
c	D _{ap} -Chr → D _{ac} -Chr	0.989	103.1 ± 2.6	95.1 ± 3.2	79.3 ± 4.4
d	CTC-D → TTC-D	0.991	64.5 ± 1.9	-59.9 ± 3.4	79.5 ± 3.7
e	Spo-D → TTC-D	0.981	69.1 ± 3.2	-41.8 ± 3.4	79.6 ± 4.7
f	TTC-D-Chr → CTC-D-Chr	0.941	41.3 ± 2.0	-167.0 ± 41.3	83.1 ± 4.4
g	Spo-D-Chr → Spo-D-TC	0.978	72.3 ± 2.5	-46.3 ± 3.1	83.9 ± 4.2
h	TTC-D-Chr → Spo-D-Chr	0.970	55.3 ± 4.4	-116.4 ± 25.2	84.4 ± 7.1
i	TTC-D → CTC-D	0.985	62.1 ± 3.2	-92.6 ± 11.3	85.3 ± 5.1
j	D _{ac} -Chr → D _{ac} -TC	0.982	82.2 ± 3.4	-14.2 ± 1.0	85.8 ± 4.8
k	TTC-D → Spo-D	0.964	56.6 ± 1.6	-119.0 ± 9.7	86.4 ± 3.5
l	TTC-D-Chr → TTC-D-TC	0.989	81.6 ± 1.5	-24.2 ± 0.8	87.7 ± 4.3

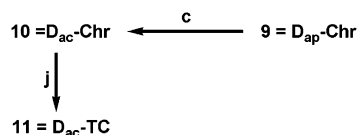
^a *r*²: Regression coefficient of the corresponding linear Eyring plot.

SCHEME 7: Photoisomers of Spo-Z Bearing a Dihydrophenanthrenic Bridge (D-bridge)^a



^a The metastable antiperiplanar D_{ap}-Chr (9) and the more stable anticlinal D_{ac}-Chr (10) were optimized using PM-3 calculations.

SCHEME 8: Mechanistic Model of the Irreversible Isomerization Paths between the Three Cyclized Isomers of Z-Chr^a



^a Letters refer to Tables 4 and 5.

with a slope of the same order of magnitude as the increase in D_{ac}-TC (Scheme 8).

Results of the kinetic analysis performed at different temperatures in the 248 to 273 K range indicated the presence of only two consecutive reactions: D_{ap}-Chr → D_{ac}-Chr and

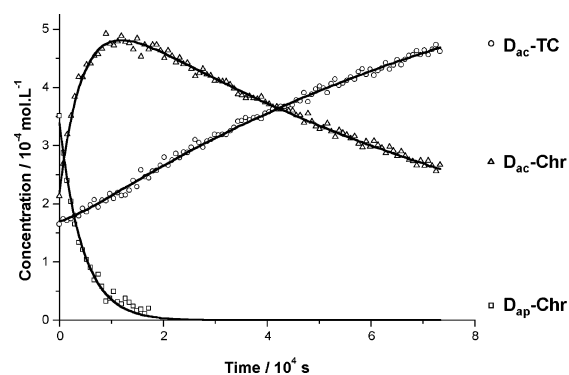


Figure 5. Thermal evolution of the three cyclized photoproducts obtained from irradiation of Z-Chr at 253 K. Signs are experimental data; continuous lines are fitted curves from the model (see Scheme 8).

D_{ac}-Chr → D_{ac}-TC, and confirmed the irreversible naphthopyran ring opening (Table 4). No direct pathway: D_{ap}-Chr → D_{ac}-TC was found. The activation parameters will be discussed below. The metastability of the antiperiplanar isomer can be interpreted from PM3 and PM3-AMSOL calculations giving rise to an energy difference between the two conformers lying between 28 and 32.7 kJ·mol⁻¹, respectively.

Comparison of the Activation Parameters of the Various Processes. The whole set of activation parameters was determined from Eyring plots ($\ln k_{ij}/T$ vs $1/T$). Table 5 shows some interesting features.

Examination of these results shows that some kinetic processes exhibit similar activation parameters independent of the

molecule where they occur. For instance, the TTC to Spo ring closure (rows h and k) is characterized in both cases by an activation enthalpy (ΔH^\ddagger) ranging from 55 to 57 kJ·mol⁻¹ and an entropy of activation (ΔS^\ddagger) from -119 to -116 J·mol⁻¹·K⁻¹ for both TTC-D-Chr and TTC-D molecules. These reactions are reversible and in both cases there is no direct path between Spo and CTC. The spirooxazine unit ring opening gives rise first to the TTC photomerocyanine, which is then thermally isomerized into its CTC isomer. On the other hand, there is an equilibrium between the CTC and TTC isomers (rows a,f and d,i). For the four reversible processes that have been detected, the free enthalpy ΔG^0 of the corresponding thermodynamic equilibrium can be estimated from the activation parameters. For instance, considering an A \rightarrow B (forward) and B \rightarrow A (reverse) equilibrium, $K_{eq} = B/A = \exp(-\Delta G^0/RT)$, we obtain:

$$\Delta G^0 = \Delta G^\ddagger(\text{forward}) - \Delta G^\ddagger(\text{reverse}) = (\Delta H^\ddagger_f - \Delta H^\ddagger_r) - T(\Delta S^\ddagger_f - \Delta S^\ddagger_r) \quad (2)$$

From eq 2, the relative stabilities of the various isomers can be compared. For both Spo-D-Chr and Spo-D molecules similar energy differences between the various isomers have been found. For instance, at 250 K, from rows h+b and rows k+e, ΔG^0 (TTC \leftrightarrow Spo) \approx +6 kJ·mol⁻¹ and from rows f+a and rows i+d ΔG^0 (TTC \leftrightarrow CTC) \approx +5 kJ·mol⁻¹ indicate the following order of relative stabilities: TTC > CTC > Spo.³⁷ The same trend (i.e., the open forms are more stable than the corresponding closed Spo) has been confirmed from PM-3 AMSOL calculations for these two compounds, although this comparison cannot be taken further due to insufficient accuracy of both activation parameter estimations and theoretical calculations.

Another example of similar behavior between parent molecules is related to the Chr \rightarrow TC, the kinetic process of the opening of the naphthopyran ring which features $\Delta H^\ddagger \approx$ 82 kJ·mol⁻¹ and $-24 < \Delta S^\ddagger < -14$ J·mol⁻¹·K⁻¹ for both TTC-D-Chr and D_{ac}-Chr compounds (rows l and j) and $\Delta H^\ddagger \approx$ 72 kJ·mol⁻¹ with $\Delta S^\ddagger \approx -46$ J·mol⁻¹·K⁻¹ for Spo-D-Chr (row g). In all cases, the naphthopyran ring opening leads irreversibly to the TC isomer. Although the antiperiplanar and anticlinal dihydrophenanthrenic stereoisomers are not systematically detected, as Ortica et al. also reported,³⁸ an antiperiplanar to anticlinal isomerization was observed in the closed naphthopyran-model compound D-Chr. However, such isomerization is expected to be rapid owing to the large positive activation entropy (row c).

An interesting property of Spo-D-TC (3) or TTC-D-TC (5) compounds is the unexpected lack of spirooxazine isomerization when the naphthopyran unit is opened. This feature is likely to be related to the fact that in the Spo-D-Chr polyphotochromic molecule the spirooxazine isomerizations are characterized by highly negative activation entropies (from -105.8 to -167 J·mol⁻¹·K⁻¹; rows a, b, f and h) indicating the need for some organizational order to occur. It is likely that open naphthopyran added vibrational degrees of freedom to the molecule, and, consequently, inhibited the spirooxazine unit from finding the right path to reach the transition states of isomerization.

Conclusion

During the multistep thermal relaxation recorded after UV irradiation of the Spo-Z-Chr molecule bearing both a spirooxazine and a naphthopyran unit, five interconverting electrocyclic isomeric structures (Spo-D-Chr (1), TTC-D-Chr (2), Spo-D-TC (3), CTC-D-Chr (4), and TTC-D-TC (5)) were detected using ¹H and ¹⁹F NMR spectroscopy. The complex dark

relaxation of these photoinduced isomer molecules was investigated at different temperatures. Two model compounds, namely a spironaphthoxazine linked to a 2-methoxynaphthalene (Spo-Z) and the corresponding naphthopyran (Z-Chr), were also investigated for comparison purposes.

By numerical kinetic fitting of the concentration vs time kinetic curves, it was shown that the spirooxazine units undergo thermochromic pseudo-equilibrium between the closed (Spo-) and the two transoid-cis (TTC- and CTC-) photomerocyanines. It was proved that the CTC isomer did not close directly, but isomerized reversibly to the TTC which, in turn, isomerized reversibly to the closed form (Spo-). The naphthopyran unit (-Chr) led to only one permanent open form (-TC), whereas, in the naphthopyran model, this transoid-cis isomer resulted from the opening of the anticlinal conformer (D_{ac}-Chr) itself resulting from a rapid conversion of the antiperiplanar one (D_{ap}-Chr). An unexpected property of the photocyclized Spo-D-Chr molecule was the complete inhibition of thermochromic pseudo-equilibrium between closed (Spo-) and both transoid-cis merocyanines (TTC- and CTC-) after the irreversible ring-opening of the naphthopyran moiety.

Acknowledgment. The 300 MHz NMR facilities were funded by the Région Nord-Pas de Calais (France), the Ministère de la Jeunesse, de l'Éducation Nationale et de la Recherche (MJENR), and the Fonds Européens de Développement Régional (FEDER). Part of this collaborative work was performed within the framework of the "Groupe de Recherche: Photochromes Organiques, Molécules, Mécanismes, Modèles", GDR CNRS no. 2466. J.C.M. and A.M. are also grateful to the INTAS program (00152). We thank Dr. V. Lokshin (UMR CNRS 6114, University of Méditerranée) for the synthesis of Spo-Z-Chr, Spo-Z, and Z-Chr.

Supporting Information Available: ¹H NMR spectra, Eyring plots of Spo-D and Chr-D, and details about PM3 calculations (pdf). This material is available free of charge via the Internet at <http://pubs.acs.org>.

References and Notes

- Irie, M. *Photoreactive Materials for Ultrahigh-Density Optical Memory*; Elsevier: Amsterdam, 1994.
- Irie, M. *Chem. Rev.* **2000**, *100*, 1685–1716.
- Delaire, J. A.; Nakatani, K. *Chem. Rev.* **2000**, *100*, 1817–1845.
- Yi, T.; Sada, K.; Sugiyasu, K.; Hatano, T.; Shinkai, S. *Chem. Commun.* **2003**, 344–345.
- Photochromism: Molecules and Systems*; Dürr, H., Bouas-Laurent, H., Eds.; Elsevier: Amsterdam, 1990.
- Organic Photochromic and Thermodynamic Compounds*; Crano, J. C., Guglielmetti, R. J., Eds.; Kluwer Academic/Plenum Publishers: New York, 1999; Vols. 1 and 2.
- Maeda, S. In *Organic Photochromic and Thermodynamic Compounds*; Crano, J. C., Guglielmetti, R. J., Eds.; Kluwer Academic/Plenum Publishers: New York, 1999; Vol. 1, p 85–107.
- Chu, N. Y. C. In *Photochromism: Molecules and Systems*; Dürr, H., Bouas-Laurent, H., Eds.; Elsevier: Amsterdam, 1990; pp 493–508, pp 879–882.
- Becker, R. S.; Michl, J. *J. Am. Chem. Soc.* **1966**, *88*, 5931–5933.
- Van Gemert, B. In *Organic Photochromic and Thermochromic Compounds*; Crano, J. C., Guglielmetti, R. J., Eds.; Kluwer Academic/Plenum Publishers: New York, 1999; Vol. 1, p 111–140.
- Gautron, R. French Patent (Saint Gobain) 1,450,583 and 1,451,583, 1966.
- Ribes, F.; Guglielmetti, R.; Metzger, J. *Bull. Soc. Chim. Fr.* **1972**, *1*, 143–147.
- Zhao, W.; Carreira, E. M. *J. Am. Chem. Soc.* **2002**, *124*, 1582–1583.
- Samat, A.; Lokshin, V.; Chamontin, K.; Levi, D.; Pepe G.; Guglielmetti, R. *Tetrahedron* **2001**, *57*, 7349–7359.
- Mixing of blue open spirooxazine and red open naphthopyran produces a neutral gray color, adequate for commercially acceptable

ophthalmic lenses. See: Crano, J.; Flood, T.; Knowles, D.; Kumar, A.; Van Gemert, B. *Pure Appl. Chem.* **1996**, *68*, 1395–1398.

(16) Tamai, N.; Miyasaka, H. *Chem. Rev.* **2000**, *100*, 1875–1890.

(17) Muzkat, K. A.; Eisenstein, M.; Fischer, E.; Wagner, A.; Ittah Y.; Lüttke, W. *J. Am. Chem. Soc.* **1997**, *119*, 9351–9360.

(18) Jockush, S.; Turro N. J.; Blackburn, F. R. *J. Phys. Chem. A* **2002**, *106*, 9236–9241.

(19) Ortica, F.; Levi, D.; Brun, P.; Guglielmetti, R.; Mazzucato U.; Favaro, G. *J. Photochem. Photobiol. A: Chem.* **2001**, *139*, 133–141.

(20) Berthet, J.; Delbaere, S.; Levi, D.; Brun, P.; Guglielmetti, R.; Vermeersch, G. *J. Chem. Soc., Perkin Trans. 2* **2002**, *12*, 2118–2124.

(21) Samat, A.; Lokshin, V. In *Organic Photochromic and Thermochromic Compounds*; Crano, J. C., Guglielmetti, R. J., Eds.; Kluwer Academic/Plenum Publishers: New York, 1999; Vol. 2, p 415–460.

(22) Koumura, N.; Zijlstra, R. W. J.; Van Delden, R. A.; Harada, N.; Feringa, B. L. *Nature* **1999**, *401*, 152–155.

(23) Delbaere, S.; Micheau, J. C.; Teral, Y.; Bochu, C.; Campredon, M.; Vermeersch, G. *Photochem. Photobiol.* **2001**, *74*, 694–699.

(24) Delbaere, S.; Luccioni-Houze, B.; Bochu, C.; Teral, Y.; Campredon, M.; Vermeersch, G. *J. Chem. Soc., Perkin Trans. 2* **1998**, 1153–1158.

(25) Delbaere, S.; Bochu, C.; Azaroual, N.; Buntinx, G.; Vermeersch, G. *J. Chem. Soc., Perkin Trans. 2* **1997**, 1499–1501.

(26) Kaps, K.; Rentrop, P. *Comput. Chem. Eng.* **1984**, *8*, 393–396.

(27) Minoux, M. In *Programmation Mathématique*; Dunod, Ed.; Bordas: Paris, 1983; p 95–168.

(28) Deniel, M. H.; Lavabre, D.; Micheau, J. C. In *Organic Photochromic and Thermodynamic Compounds*; Crano, J. C., Guglielmetti, R. J., Eds.; Kluwer Academic/Plenum Publishers: New York, 1999; Vol. 2, p 167–209.

(29) Matsen, F. A.; Franklin, J. L. *J. Am. Chem. Soc.* **1950**, *72*, 3337–3341.

(30) Stewart, J. J. P. *J. Comput. Chem.* **1989**, *10*, 209. (b) Stewart, J. J. P. MOPAC 7.0: A Semiempirical Molecular Orbital Program, No. 455, Quantum Chemistry Program Exchange (QCPE), Indiana University, Bloomington, IN 47405.

(31) AMSOL v. 6.6. Hawkins, G. D.; Giesen, D. J.; Lynch, G. C.; Chambers, C. C.; Rossi, I.; Storer, J. W.; Li, J.; Zhu, T.; Winget, P.; Rinaldi, D.; Liotard, D. A.; Cramer, C. J.; Truhlar, D. G. (b) Cramer, C. J.; Truhlar, D. G. *J. Comput. Aid. Mol. Design* **1992**, *6*, 629–666. (c) Chambers, C. C.; Giesen, D. J.; Gu, M. Z.; Cramer, C. J.; Truhlar, D. G. *J. Phys. Chem.* **1997**, *101*, 2061–2069.

(32) Details about the characterization are reported in the Supporting Information.

(33) To simplify and homogenize the names of all the different structures, we have applied the following nomenclature: Spo is related to the spirooxazine entity in closed configuration. TTC (Trans–Transoid–Cis) and CTC (Cis–Transoid–Cis) are related to the isomerism of opened spirooxazine. Chr is related to the naphthopyran entity in closed configuration. TC (Transoid–Cis) is related to the isomerism of opened naphthopyran. Z characterizes the isomerism of ethenic spacer, while D is related to the dihydrophenanthrenic nucleus. For instance, TTC-D-TC indicates that the spirooxazine is opened in the TTC isomerism, the naphthopyran is opened in the TC isomerism, and that the Z-ethenic bridge has been electrocyclicized (D).

(34) $\ln(k_{ij}/T) = \ln(k_B/h) + \Delta S^\ddagger/R + \Delta H^\ddagger/RT$ (k_{ij} represents the corresponding first-order rate constant of isomerization of compound i to compound j , k_B is Boltzmann's constant, h is the Planck's constant ($\ln(k_B/h) = 23.76$), and R is the gas constant.

(35) Berthet, J.; Delbaere, S.; Lokshin, V.; Bochu, C.; Samat, A.; Guglielmetti R.; Vermeersch, G. *Photochem. Photobiol. Sci.* **2002**, *1*, 333–339. Berthet, J.; Delbaere, S.; Lokshin, V.; Samat A.; Vermeersch, G. *Photochem. Photobiol. Sci.* **2003**, *2*, 978–980.

(36) Berthet, J.; Delbaere, S.; Levi, D.; Samat, A.; Guglielmetti, R.; Vermeersch, G. *Photochem. Photobiol. Sci.* **2002**, *1*, 665–672.

(37) Hobbey J.; Malatesta V. *Phys. Chem. Chem. Phys.* **2000**, *2*, 57–59.

(38) Ortica, F.; Levi, D.; Brun, P.; Guglielmetti, R.; Favaro G.; Mazzucato, U. *Intern. J. Photoenergy* **2001**, *3*, 153–160.